APPENDIX

APPENDIX

CONTENTS

APPENDIX

LIST OF FIGURES AND TABLES

(FIGURE)

(TABLE)

A-1 Detailed geological mapping

A.1.1 Method for plotting fracture orientation

The orientation (dip and strike) of a fracture was described by plotting the pole of the fracture on the projection plane using a Wullf-stereonet.

As shown in the following figure (A) a perpendicular line from the center (0) of the plane of fracture to the surface of the hemisphere (T) is drawn. This point (T) shows the pole of the fracture.

The pole is plotted on the projection plane by first drawing a line perpendicular to the strike of the fracture (dashed line in figure (B)). From the great circle of the fracture on the projection plane count 90° along the perpendicular line (dashed line). The point gives the pole of the fracture (S).

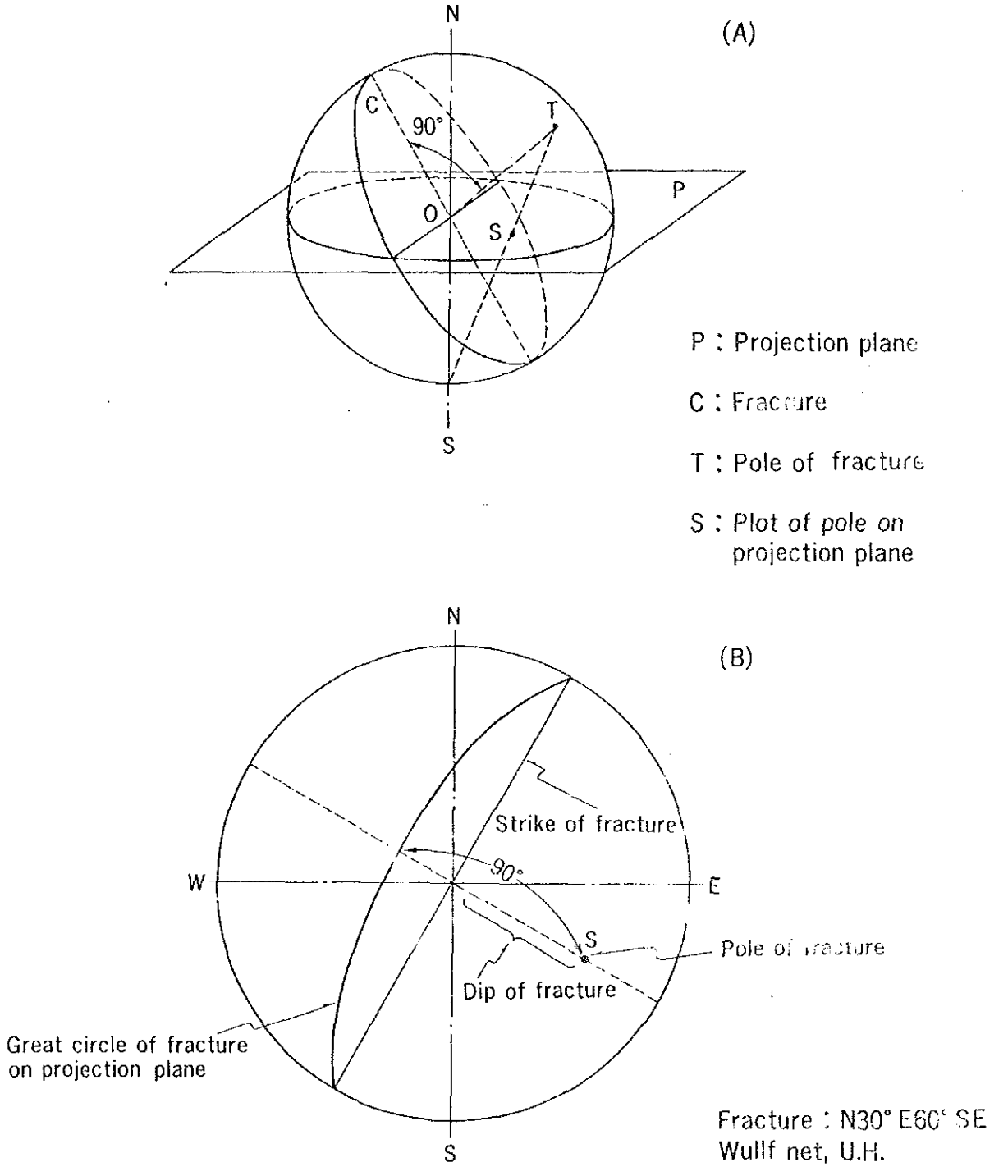

Fig. A.1.1 Method for plotting fracture orientation

A.1.2 Method for making contour diagram

The drawing of the contour diagram is as follows:

(1) A point diagram is covered with a grid as shown in the following figure.

(2) A counting circle of fixed area is placed at the center of each grid point.

(3) The number of poles in the counting circle are counted and are expressed as a percentage.

(4) According to the value of each grid point, a controur line is drawn.

When the general directions of fractures are seen, a large area counting circle is used and when the detailed concentration of fractures are seen, a small area counting circle is used.

The computer program "POLE-CONT. BAS" (1987, YAMANE, et al., Osaka City University) was used in drawing the point and contour diagram.

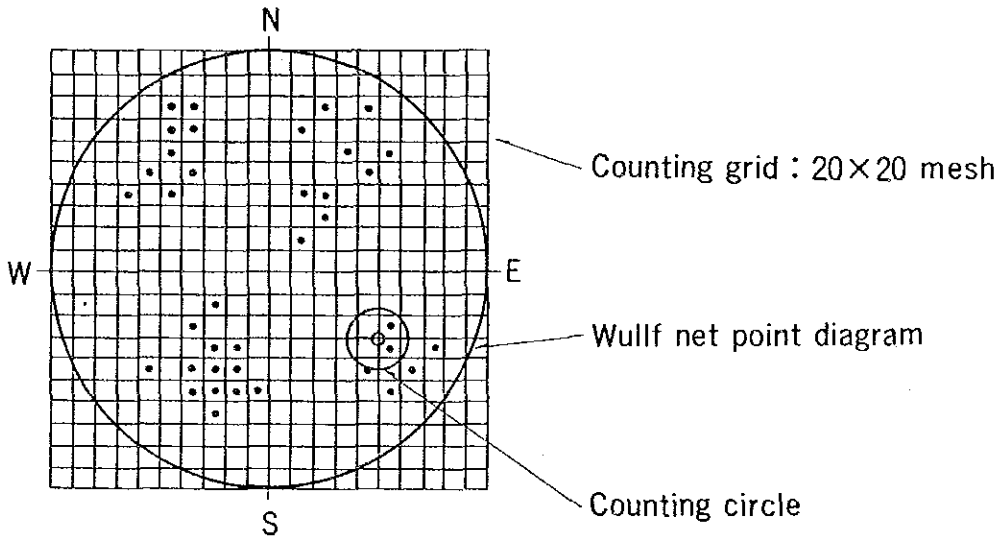

Fig. A.1.2 Method for making contour diagram

A.1.3 Presumption of stress field

The stress field can be expressed using three axis of principal stress; maximum (1), intermediate (2) and minimum (3) which fall at right angles to each other. The presumption method of the stress field and the relation between the fault and the axis of principal stress are as follows:

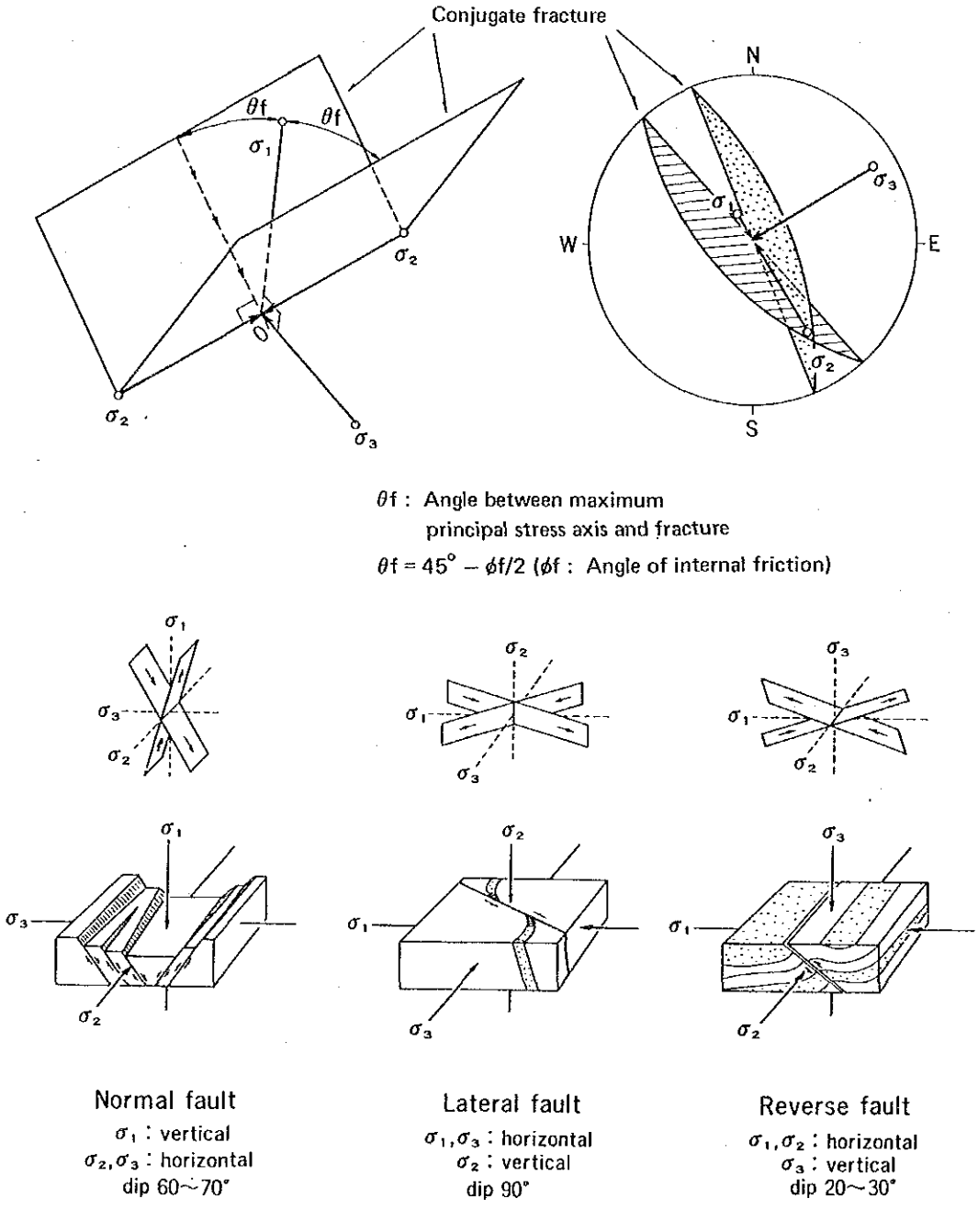

Fig. A.1.3 Presumption of stress field and relation between fault and axis of principal stress (Anderson, 1951)

A.2 CSAMT survey

A.2.1 Survey lines and points

Leveling work for survey lines and points was under taken by MTA. Line number and the locations are shown in Table A.2.1 and Fig. A.2.1.

Table A.2.1 Survey lines and points

Line	Point Number	No.
A	100, 300, 500, 700, 900, 1,100, 1,200, 1,300 1,400, 1,500, 1,600, 1,700, 1,900, 2,000, 2,100, 2,200 2,300, 2,400 2,600 2,800, 3,000, 3,200, 3,400	23
B	50, 150, 250, 350, 450, 550, 650, 750 850, 950, 1,050, 1,150, 1,250, 1,350	14
C	100, 300, 500, 700, 900, 1,100, 1,200, 1,300 1,400, 1,500, 1,600, 1,700, 1,800, 1,900, 2,000, 2,100 2,200, 2,300, 2,400, 2,600, 2,800, 3,000, 3,200, 3,400	24
D	50, 150, 250, 350, 450, 550, 650, 750 850, 950, 1,050, 1,150, 1,250, 1,350	14
E	100, 300, 500, 700, 900, 1,100, 1,200, 1,300 1,400, 1,500, 1,600, 1,700, 1,800, 1,900, 2,000, 2,100 2,200, 2,300, 2,400, 2,600, 2,800, 3,000, 3,200, 3,400	24
F	50, 150, 250, 350, 450, 550, 650, 750 850, 950, 1,050, 1,150, 1,250, 1,350	14
G	100, 300, 500, 700, 900, 1,100, 1,200, 1,300 1,400, 1,500, 1,600, 1,700, 1,800, 1,900, 2,000, 2,100 2,200, 2,300, 2,400, 2,600, 2,800, 3,000, 3,200, 3,400	24
H	50, 150, 250, 350, 450, 550, 650, 750 850, 950, 1,050, 1,150, 1,250, 1,350	14
I	100, 300, 500, 700, 900, 1,100, 1,200 1,300 1,400, 1,500, 1,600, 1,700, 1,800, 1,900, 2,000, 2,100 2,200, 2,300, 2,400, 2,600, 2,800, 3,000, 3,200, 3,400	24

Line	Point Number	No.
J	50, 150, 250, 350, 450, 550, 650, 750, 850, 950, 1,050, 1,150, 1,250, 1,350	14
K	100, 300, 500, 700, 900, 1,100, 1,200, 1,300 1,400, 1,500, 1,600, 1,700, 1,800, 1,900, 2,000, 2,100 2,200, 2,300, 2,400, 2,600, 2,800, 3,000, 3,200, 3,400	24
L	50, 150, 250, 350, 450, 550, 650, 850 950, 1,050, 1,150, 1,250, 1,350	13
M	100, 300, 500, 700, 900, 1,100, 1,200, 1,300 1,400, 1,500, 1,600, 1,700, 2,000, 2,100, 2,200, 2,300 2,400, 2,600, 2,800, 3,000, 3,200, 3,400	22
N	50, 150, 250, 350, 450, 550, 950, 1,050 1,150, 1,250, 1,350	12
O	100, 300, 500, 700, 900, 1,100, 1,200, 1,300 1,400, 1,500, 1,600, 1,700, 2,000, 2,100, 2,200, 2,300 2,400, 2,600, 2,800, 3,000, 3,200, 3,400	22
P	50, 150, 250, 350, 650, 750, 850, 950	8
Q	100, 300, 500, 700, 900, 1,100, 1,200, 1,300 1,400, 1,500, 1,600, 1,700, 2,400, 2,600, 2,800, 3,000 3,200, 3,400	17
R	50, 150, 250, 350, 450, 550, 650, 750 850, 950, 1,050, 1,150	12
S	100, 300, 500, 700, 900, 1,100, 1,200, 1,300 1,400, 1,500, 1,600, 1,700, 1,800, 1,900, 2,000, 2,100 2,200, 2,300, 2,600, 2,800, 3,000, 3,200, 3,400	23
T	50, 150, 250, 350, 450, 550, 650, 750 850, 950, 1,050, 1,150, 1,250	13
U	100, 300, 500, 700, 900, 1,100, 1,200, 1,300 1,400, 1,500, 1,600, 1,700, 1,800, 1,900, 2,000, 2,100 2,200, 2,600, 2,800, 3,000, 3,200	21

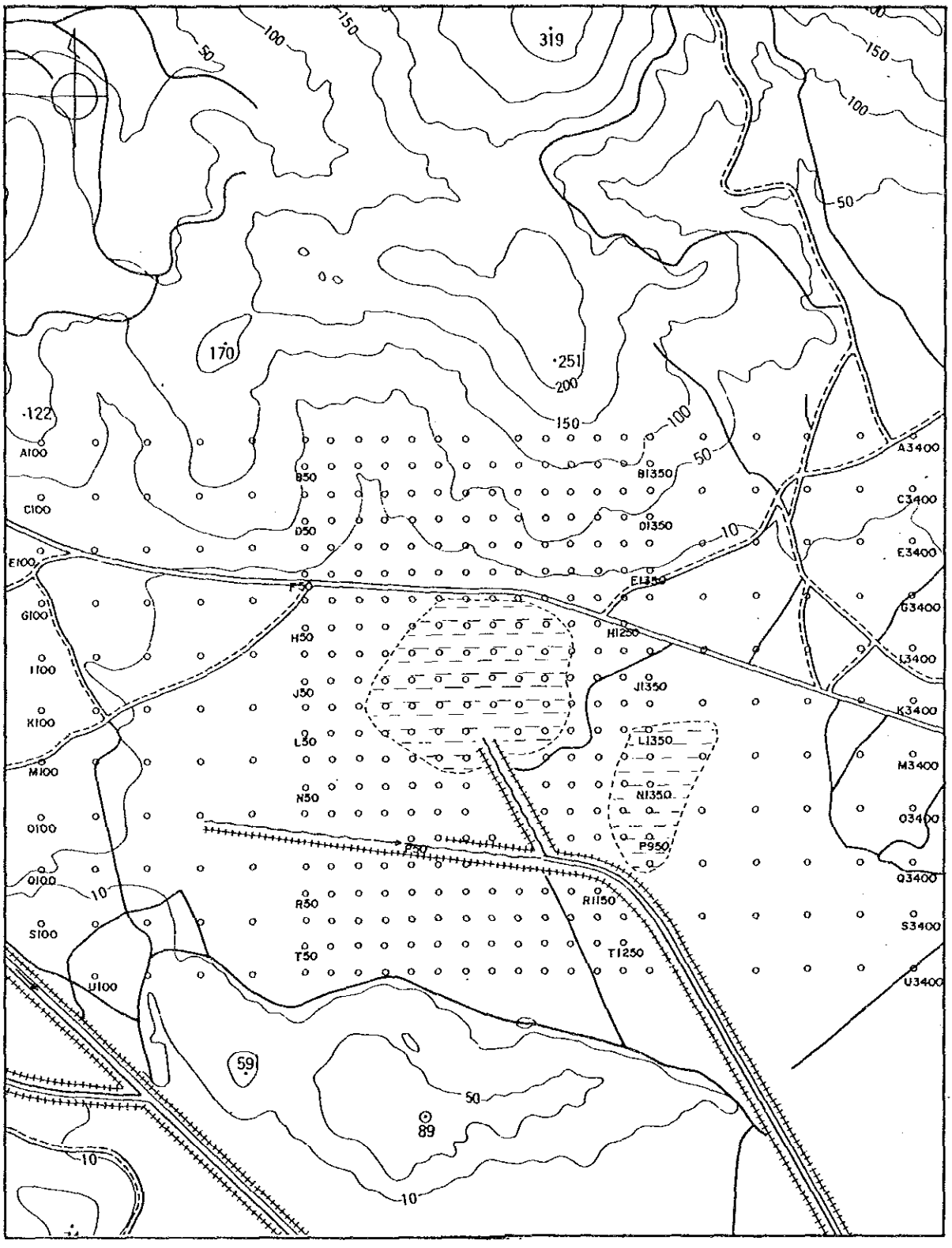

Fig. A.2.1 Survey lines and points for CSAMT measurement

A.2.2 Measuring equipment

Measuring equipment is shown in Table A.2.2. These equipment was donated by JICA to MTA for this project.

Table A.2.2 Specifications of the equipment for CSAMT survey

Equipment	Model	Manufacture	Specification
Transmitter	IPT-1	Phophisics, Inc.	Output: 10 A max., 800 V max., 60 V min., 3 kW max. Frequency: DC to 10 kHz
Motor Generator	MG-3	Phoenix Geophysics, Inc.	Output: 3 kVA max., 8 HP at 3,000 rpm
Magnetic Sensor Coil	AMT-30	Phoenix Geophysics, Inc.	Inductance: 75 Henries. 500 ohms DC resistance Sensitivity: 0.05 volts/gamma
Receiver	V-4	Phoenix Geophysics, Inc.	Dynamic range: 10 volts Frequencies: 0.0625 to 8,192 Hz in 18 binary step SP cancellation: Up to 2.5 volts automatic Notch filter: 1st, 3rd and 5th harmonic of 50 Hz or 60 Hz A-D conversion: 16 bits resolution, 10 V range Memory: 40 k bytes of EPROM 48 k bytes of RAM memory
Electrode	PE-2	Phoenix Geophysics, Inc.	Pb-$PbC1_2$ type porous pot

A.2.3 Method of analysis

1. Basic theory of CSAMT method

The apparent resistivity is calculated from the ratio of the electric field and magnetic field magnitudes using the well-known Cagniard equation for MT:

$$\rho a = \frac{1}{5f}\left|\frac{Ex}{Hy}\right|^2 \qquad (1)$$

where ρa is the apparent resistivity in ohm-m, f is the frequency in Hz, Ex is the E-field magnitude in mv/km and Hy is the H-field magnitude in gammas. It should be noted that the Cagniard equation is valid only in the plane wave configuration for the electromagnetic field; i.e., when the distance between transmitting signal source and receiving location is sufficiently large.

2. Near-field and Transition-field

In a CSAMT survey, the distance between the transmitter and receiver locations is constrained in general by the requirement that the magnetic and electric field be strong enough to permit useful measurements. The paradox is that where the "plane-wave" assumption is valid, the signal is weak; and where the signal is strongest (near the transmitter), the "plane-wave" assumption is no longer true.

At some distance from the transmitter dipole, where the transmitted electromagnetic field becomes a "plane-wave", it is called "far-field". The Cagniard equation is valid in the "far-field" situation to calculate the apparent resistivity. The far-field distance, Lf, is approximately given by the following equation:

$$Lf \geqq 3 \times \text{skin depth} \doteqdot 1{,}509\sqrt{\rho/f} \qquad (2)$$

where Lf is in meters, ρ is the resistivity of the homogeneous earth in ohm-m and f is the frequency in Hz.

If the distance between transmitter and receiver is much less than Lf, the transmitted field is not "plane-wave" in character; it is referred to as the "near-field". In the "near-field", the Cagniard equation overestimates the actual resistivity.

Fig. A.2.2 shows the apparent resistivity curve, using the Cagniard equation with theoretically calculated E_X and H_Y values, over a homogeneous earth. The apparent resistivity curve in the "near-field" is characterized by a slope of 45 degrees, meaning that the apparent resistivity value is doubled by each binary frequency step. The

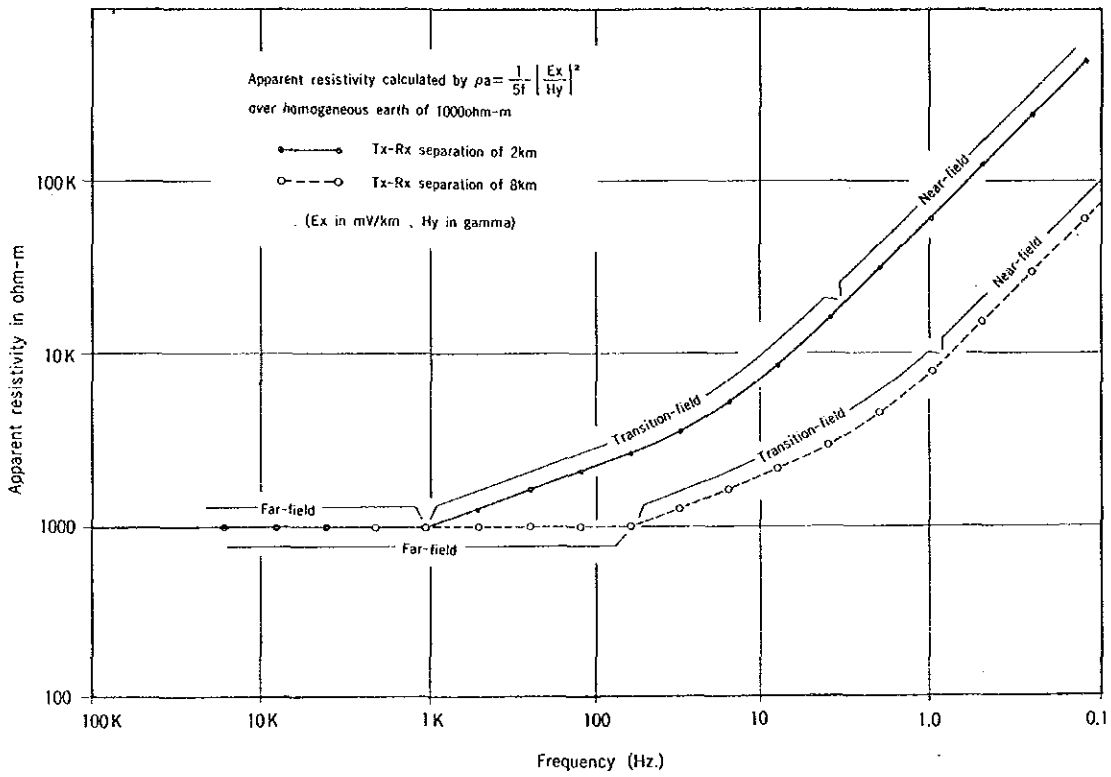

Fig. A.2.2 Apparent resistivity vs frequency calculated by Cagniard equation over homogeneous earth of 1,000 ohm-m

(1) "Near-Field" correction

A equation for apparent resistivity in a "near-field" situation is calculated as follows:

$$\rho a = K(r) \times r \times \left|\frac{Ex}{Hy}\right| \qquad (3)$$

where K(r) is a constant function of r; and r is the distance between transmitter and receiver in km. E_X and H_y are in the same units as in the Cagniard equation.

Table A.2.3 indicates the calculated value of K(r) for various distances and resistivities for the homogeneous earth. The E_X and H_y field strength values are theoretically calculated. Fig. A.2.3 shows the theoretically calculated apparent resistivity curve over a homogeneous earth, using the "near-field" equation.

Table A.2.3 K(r) value for near-field apparent resistivity formula

$$\rho a = K(r) \cdot r \cdot \left|\frac{Ex}{Hy}\right| \qquad r: \text{Tx-Rx distance in km}$$

r (km)	K 1 ohm-m	K 10 ohm-m	K 100 ohm-m	K 1,000 ohm-m	K 10,000 ohm-m	K average
.5	2.528	2.523	2.527	2.524	2.523	2.52
1.0	1.409	1.406	1.407	1.406	1.405	1.41
1.5	1.046	1.048	1.049	1.048	1.047	1.05
2.0		.890	.890	.889	.889	.889
2.5		.806	.805	.805	.805	.805
3.0		.755	.755	.756	.755	.755
3.5		.726	.724	.724	.724	.724
4.0			.702	.703	.702	.702
5.0			.676	.676	.676	.676
6.0			.661	.661	.661	.661
8.0			.646	.646	.646	.646
10.0	frequency is too low to		.642	.642	.642	.642
12.0	achieve good accuracy			.636	.636	.636
14.0	in field calcuration			.635	.635	.635
17.0	for near-field situation			.635	.634	.634
20.0					.633	.633

A comparison of the data from Fig. A.2.2 using the Cagniard equation, and Fig. A.2.3 using the "near-field" equation, shows that the calculated apparent resistivity in the "near-field" is valid in the same manner as Cagniard resistivity is valid in the "far-field". The apparent resistivity value in the "far-field" using the "near-field" equation is characterized by the slope 0.5 in the log-log plot. The perfect correlation of the "near-field" zone, the "transition-field" zone and the "far-field" zone from Fig. A.2.2 using the Cagniard equation and Fig. A.2.3 using the "near-field" equation, is shown in Fig. A.2.4. These facts indicate that the K(r) value is only a function of the distance between the transmitter and receiver. Therefore the "near-field" equation can be used in conjunction with the Cagniard equation to give a valid interpretation.

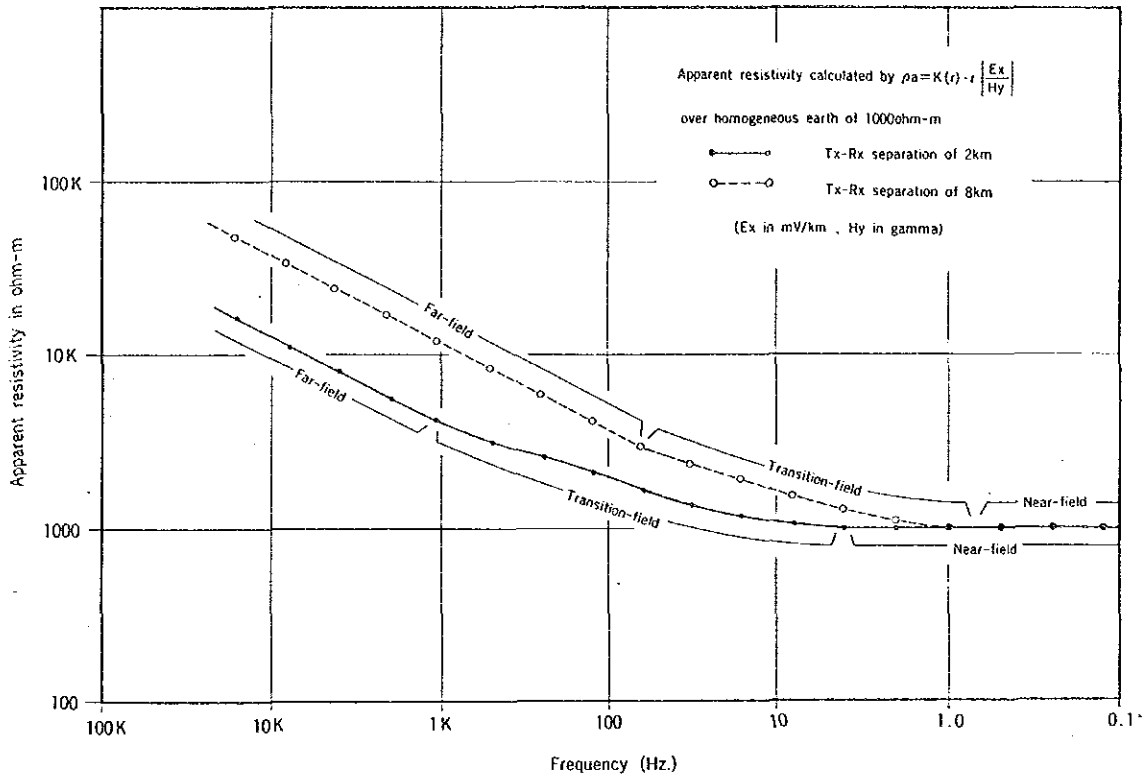

Fig. A.2.3 Apparent resistivity vs frequency calculated using "near-field" equation over homogeneous earth of 1,000 ohm-m

(2) "Transition-field" correction

The "transition field" is more complicated. The following "transition-triangle method" was used as a practical procedure.

Fig. A.2.4 indicates the triangle for various resistivities of the homogeneous earth. The "transition-triangle" pattern has a similar shape for various transmitter-receiver distances and earth resistivities. The shape is, in particular, almost identical for various resistivities, for a given transmitter-receiver distance. These facts suggest that the "transmitter-receiver distance. These facts suggest that the "transition-triangle" parameter also is a function only of the distance, and is independent of ground resistivity.

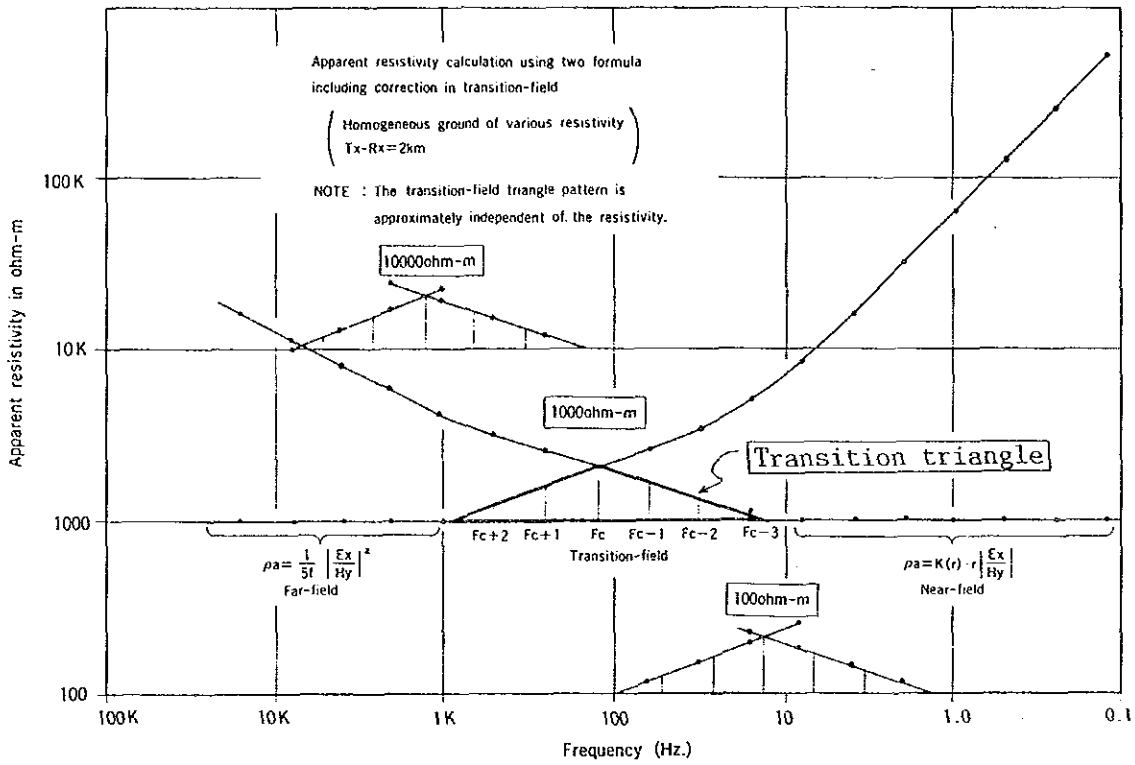

Fig. A.2.4 Homogeneous earth apparent resistivity curves. The Cagniard equation is used for the far field; "near-field" equation for near field data; and the transition triangle method to calculate resistivity in the transition zone.

Table A.2.4 indicates the triangle parameters for various distances and resistivities. Fc is the log frequency where the apparent resistivity curves of the Cagniard equation and the "near-field" equation intersect. Fc+n indicates a binary frequency step from Fc. The average slope of both sides of the triangle, for a given distance, is calculated for various resistivities.

If a proper "near-field" and "transition-field" correction is performed on CSAMT data (to obtain apparent resistivity equivalent to the 'far-field" situation), then the apparent resistivity value is equivalent to that of MT. Consequently well-developed existing interpretation techniques for MT can be utilized.

Table A.2.4 Transition triangle factor for various transmitter-receiver distance and resistivity

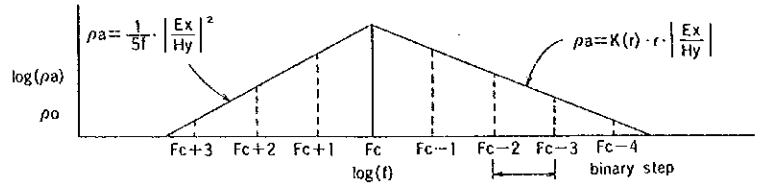

Tx-Rx	ρa / ρo Fc+5 Fc+4 Fc+3 Fc+2 Fc+1 Fc Fc−1 Fc−2 Fc−3 Fc−4 Fc−5	resistivity ρo
.5km	1.25 1.7 2.35 3.3 4.4 3.2 2.3 1.7 1.3	100 ohm-m
	1.25 1.7 2.3 3.2 4.3 3.2 2.4 1.75 1.3	1000
	1.3 1.75 2.35 3.3 4.3 3.2 2.35 1.75 1.3	10000
	.74 .74	slope
1.0km	1.2 1.6 2.15 2.85 2.2 1.73 1.35 1.04	1 ohm-m
	1.15 1.6 2.2 2.9 2.25 1.75 1.35 1.05	10
	1.2 1.6 2.15 2.8 2.2 1.7 1.3 1.0	100
	1.2 1.6 2.2 2.85 2.2 1.75 1.35 1.03	1000
	1.2 1.65 2.2 2.85 2.2 1.75 1.35 1.04	10000
	.76 .77	slope
2.0km	1.2 1.6 2.1 1.65 1.3	100 ohm-m
	1.3 1.65 2.1 1.55 1.2	1000
	1.2 1.6 2.1 1.6 1.3	10000
	.77 .77	slope
8.0km	1.3 1.75 1.35 1.15	100 ohm-m
	1.3 1.75 1.4 1.15	1000
	1.35 1.75 1.45 1.15	10000
	.78 .80	slope
20.km	1.35 1.75 1.4 1.15	100 ohm-m
	1.35 1.75 1.45 1.2	1000
	1.35 1.75 1.45 1.15	10000
	.78 .80	slope

Tx-Rx in km	.5	1.0	1.5	2.0	2.5	3.0	4.0	5.0	6.0	8.0	10.0	13.0	16.0	20.0
Interporated (ρa/ρo) at Fc	4.4	2.9	2.4	2.1	2.0	1.9	1.8	1.78	1.76	1.75	1.75	1.75	1.75	1.75

The following method was used as a calculating method of apparent resistivity.

a. Calculate apparent resistivity for each frequency using both Cagniard equation and "near-field" equations (with the appropriate transmitter-receiver distance).

b. Calculate the intersection of the two Log (ρa) vs. Log (f) curves and correct for "transition-field" by applying the "transition-triangle" method.

c. Use apparent resisitivity, calculated by the "near-field" equation for the lower frequency side fo the triangle and apparent resistivity calculated by Cagniard equation for the higher frequency portion of the curve.

3. One dimensional inversion

Impedances of the strata of horizontal strata are calculated by equation (4).

$$Z(0) = \frac{i\mu\omega}{1}\coth\left[\gamma_1 h_1 + \coth^{-1}\frac{\gamma_1}{\gamma_2}\coth\left(\gamma_2 h_2 + \coth^{-1}\frac{\gamma_2}{\gamma_3}\cdots\right.\right.$$

$$\left.\left.\cdots\coth^{-1}\frac{\gamma n\text{-}2}{\gamma n\text{-}1}\coth\left(\gamma n\text{-}1\, hn\text{-}1 + \coth^{-1}\frac{\gamma n\text{-}1}{\gamma n}\right)\cdots\right]\right)\right] \qquad (4)$$

Where, n: the number of strata
Zo: impedance of the earth measured on the ground
μ: magnetic permeability of the earth
ω: angular frequency
hn: thickness of each stratum

Impedances of the n-th stratum are expressed as follows:

$$Zn = \frac{\omega\mu}{\gamma_1}\coth\left(-i\gamma_1 h_1 + \coth^{-1}\frac{\gamma_1}{\omega\mu}\, Zn\text{-}1\right) \qquad (5)$$

$$Zn = \frac{\omega\mu}{\gamma_2}\coth\left(-i\gamma_2 h_1 + \coth^{-1}\frac{\gamma_2}{\omega\mu}\, Zn\text{-}2\right)$$

$$Z1 = \frac{\omega\mu}{\gamma n}$$

Defining Zn/Z1 = Rn, the following equation is obtained.

$$Rn = \coth -i\gamma_1 h_1 + \coth^{-1}\sqrt{\frac{\rho_2}{\rho_1}}\coth\left(-i\gamma_2 h_2 + \coth^{-1}\sqrt{\frac{\rho_3}{\rho_2}}\coth\right.$$

$$\left.\left[-i\gamma_3 h_2 + \ldots + \sqrt{\frac{\rho n\text{-}1}{\rho n\text{-}2}}\coth\left[-i\,\gamma_{-1}^{1} hn\text{-}1 + \coth^{-1}\sqrt{\frac{\rho n}{\rho n\text{-}1}}\right)\ldots\right]\right)\right] \qquad (6)$$

Where, n: $(i\sigma n\omega\mu)^{1/2}$
σn: $1/\rho n$

There is the following relation between the impedance and the resistivity.

$$\frac{\rho a}{\rho_1} = \frac{|Zn|^2}{|Z_1|^2}$$

Then, $$\rho a = \rho_1 |Rn|^2 \qquad (7)$$

Generally, apparent resistivities for each frequency are calculated by using the equations (6) and (7), and giving the initial values of ρ_1 and h_1.

Final values of resistivity and thickness of each stratum are determined by iterating the calculation to minimize the value of $i[\log(\rho_{observed})i - \log(\rho_{calculated})i]^2$.

A.3 Mise-á-masse survey

A.3.1 Survey lines and points

Leveling work for the setting lines and points was undertaken by MTA. The numbers and locations are shown in Table A.3.1 and Fig. A.3.1.

Table A.3.1 Station lines and numbers for Mise-á-la-masse survey

Line	Point Number	No.
A	1, 2, 3, 4, 5, 6, 7, 8,	8
B	9, 10, 11, 12, 13,	5
C,	14, 15, 16, 17, 18, 19	6
D	20, 21, 22, 23, 24	5
E	25, 26, 27, 28, 29, 30, 31	7
F	32, 33, 34, 35, 36	5
G	37, 38, 39, 40, 41, 42	6
H	43, 44, 45, 46, 47	5
I	48, 49, 50, 51, 52, 53, 54, 55	8
J	56, 57, 58, 59, 60	5
K	61, 62, 63, 64, 65, 66	6
L	67, 68, 69, 70, 71	5
M	72, 73, 74, 75, 76, 77, 78	7
N	79, 80, 81, 82, 83	

Line	Point Number	No.
O	84, 85, 86, 87, 88, 89	6
P	90, 91, 92, 93, 94	5
Q	95, 96, 97, 98, 99, 100, 101, 102	8
R	103, 104, 105, 106, 107	5
S	108, 109, 110, 111, 112, 113	6
T	114, 115, 116, 117, 118	5
U	119, 120, 121, 122, 123, 124, 125	7
V	126, 127, 128, 129, 130	5
W	131, 132, 133, 134, 135, 136	6
X	137, 138, 139, 140, 141	5
Y	142, 143, 144, 145, 146, 147, 148, 149	8
Z	150, 151, 152, 153, 154	5
AA	155, 156, 157, 158, 159, 160	6
BB	161, 162, 163, 164, 165	5
CC	166, 167, 168, 169, 170, 171, 172	7
DD	173, 174, 175, 176, 177	5
EE	178, 179, 180, 181, 182, 183	6
FF	184, 185, 186, 187, 188	5

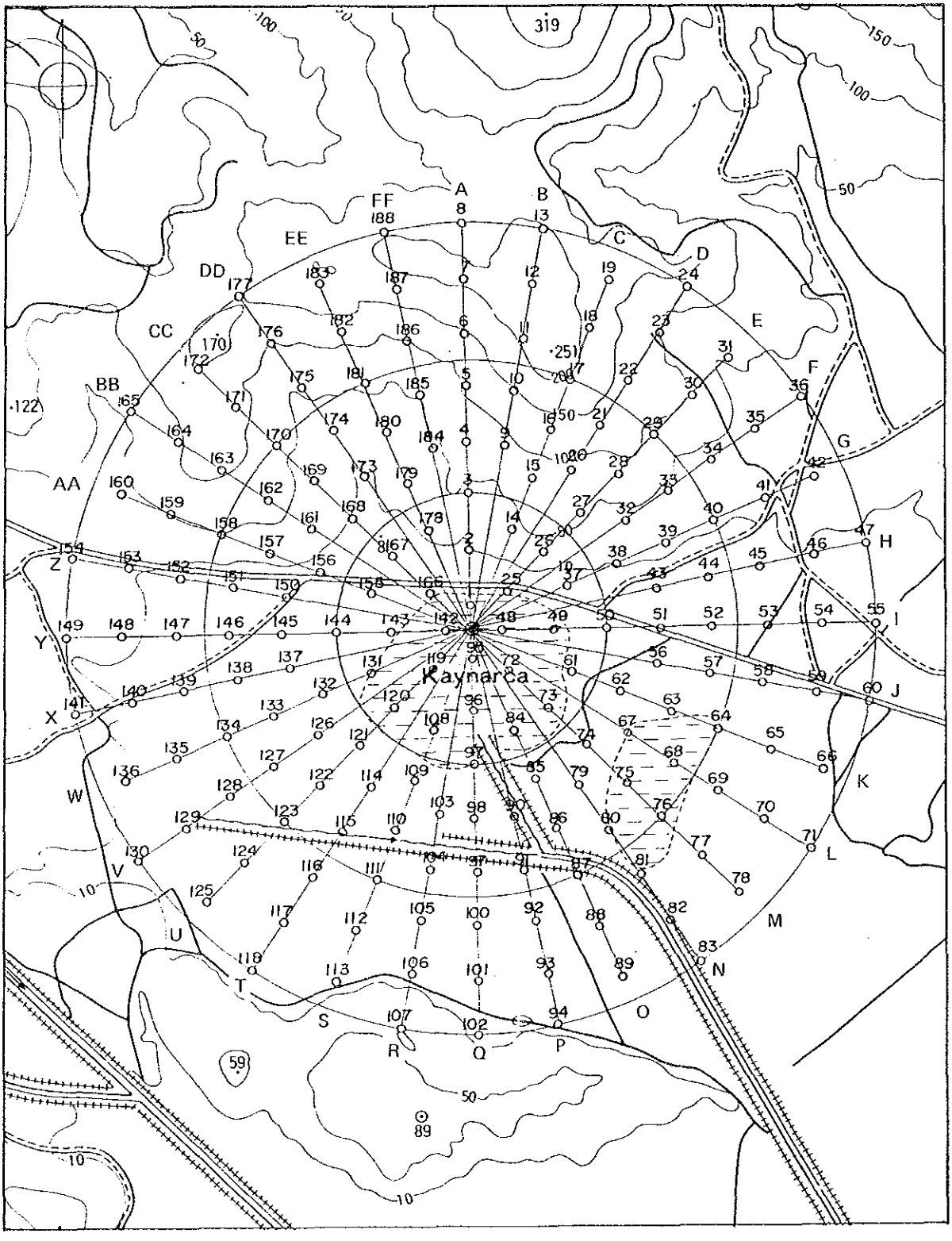

Fig. A.3.1 Survey lines and points for Mise-á-la-masse survey

A.3.2 Measuring equipment

Measuring equipment is shown in Table A.3.2.

Table A.3.2 Specifications of the measuring equipment for Mise-á-la-masse survey

Equipment	Model	Manufacture	Specification
Transmitter			
IP transmitter	IPT-1	Phoenix Geophysics, Inc.	Output: 900 V, 10 A 3 kVA max.
Engine generator	MG-3	Phoenix Geophysics, Inc.	Output: 45 – 75 V, 3 kVA
Recorder	EPR-100A	Towa Denpa	±1 mV to 100 V
Standard resistor		Yokogawa Denki	1 ohm
Receiver			
Recorder	EPR-100A	Towa Denpa	±1 mV to 100 V
Prefilter	YI5606	Yokohama Denshi	

A.3.3 Method of analysis

1. Basic conception of the method

The resistivity of rocks is strongly affected by the porosity, electrolytes and temperature rather than the rock type. When a Schlumberger array is used, the low resistivity zone does not represent layers and/or faults of a geothermal reservoir but usually shows the altered zone overlying the geothermal reservoir. It has been recently accepted that the resistivities of fractured reservoirs and aquifers are higher than that of altered zones.

It does not always follow that a low resistivity zone coincides with the extent of a geothermal reservoir. So that the result of electric exploration using the schlumberger array should be discussed carefully with the aid of other data such as geology and geochemistry.

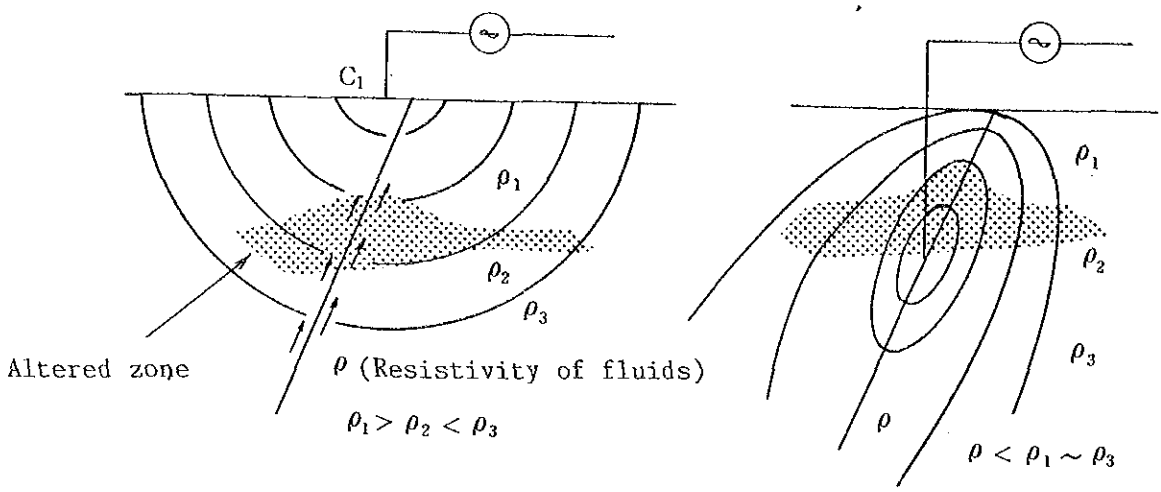

(1) Electrode located at the earths surface (Schlumberger method)

(2) Mise-á-la-masse method

Fig. A.3.2 The shape of the electric around a current electrode

2. Data processing method

The voltage difference between P1 and P2 was calculated by the following equation,

$$V_{(i)} = \frac{V_{P1P2\,(i)}}{V_{P2P2'(i)}} \times \frac{V_{P1P2'/188}}{V_{P1P2/188}}$$

Where,

$V_{p1P2(i)}$:	voltage difference between P1 and P2 at station i
$V_{P2P2'(i)}$:	voltage difference between P2 and P2' at station i
$V_{P1P2/188}$:	mean value of all voltage differences between P1 and P2
$V_{P1P2'/188}$:	mean value of all voltage differences between P2 and P2'
V(i):	corrected voltage difference value between P1 and P2
(i):	number of station

The corrected value V(i) and measured current I(i) were used to calculate the apparent resistivity by the following formula:

$$\rho a(i) = 2\pi \frac{V(i)}{I(i)} / F(PiCj, L) \qquad (1)$$

Where,

ρa(i):	apparent resistivity for station i (ohm-m)
F(PiCj, L):	theoretical potential (l/m)

and

$$F(PiCj, L) = \frac{1}{L} \cdot \log \frac{(L+HP1C1+\sqrt{P1C1^2+(L+HP1C1)^2})(HP2C1+\sqrt{P2C1^2+HP2C1^2})}{(L+HP2C1+\sqrt{P2C1^2+(L+HP2C1)^2})(HP1C1+\sqrt{P1C1^2+HP1C1^2})} - \frac{1}{P1C2} + \frac{1}{P2C2} \quad (2)$$

Where, L: line source length (m)

PiCj (i=1, j=1, 2): distance between current electrode and potential electrode

HPiCj (i=1, 2: j=1, 2) elevation difference between current electrode and potential electrode
(Elevation of Pi minus elevation of Ci)

To calculate the apparent resistivity for each station, the theoretical potential is used to delineate effects by the current electrode array and the topographical conditions.

Usually apparent resistivities obtained by Mise-á-la-masse surveys have tendencies to increase or decrease the values by increasing the distance between a near current electrode and a movable potential electrode. Residual apparent resistivities are calculated by the following formula.

$$\Delta\rho a(i) = \rho a(i) - \rho_{cal}(i)$$

$$= 2\pi \frac{V(i)}{I(i)} /F(PiCj, L) - F(d) \quad (3)$$

Where, $\Delta\rho a(i)$: residual apparent resistivity

$\rho a(i)$: apparent resistivity calculated by equation

$$\rho_{cal}(i) = F(d) \quad (4)$$

Where, F(d): average apparent resistivity calculated by the least square method

A.4 Thermal gradient survey

A.4.1 Calculation of static formation temperature

For estimating the static formation temperature, the following formulas are used. It is assumed that the temperature at a certain depth would be cooled by water circu-

lation and would recover its temperature to the initial level with the passing of time after stopping the circulation.

$$Tf = a + b \ln (b \times 100 + 1)$$

Tf: static formation temperature

$$a = \overline{T} - b\overline{h}$$

$$b = Sxy/Sx$$

$$\overline{T} = \frac{1}{N} \sum_{i=1}^{N} Ti$$

$$\overline{h} = \frac{1}{N} \sum_{i=1}^{N} \ln hi$$

$$Sx = \sum_{i=1}^{N} (\ln hi - \overline{h})$$

$$Sxy = \sum_{i=1}^{N} (\ln hi - \overline{h})(Ti = \overline{T})$$

Ti: Temperature at time i i=1, 2 3, ..., N

hi: ith time (hrs)

A.4.2 Calculation of heat flow

For estimating the heat flow, the following formulas were used.

$$Q = K\frac{\partial T}{\partial Z}$$

Where, K: thermal conductivity of rock (cal/cm. sec.°C)

$\frac{\partial T}{\partial Z}$: thermal gradient

Q: heat flow (cal/cm^2.sec)

A.4.3 Method of X-ray analysis

In order to know the characteristics and degree of hydrothermal alteration, altered zones were evaluated using the concept of the classification of alteration type and the quartz index. Their principles are outlined below.

(1) Quartz index (QI)

The quartz index of a mineral in a sample is represented by the percentage of the strongest X-ray intensity of the mineral, Im (cps), to that of pure quartz, Iq (cps), measured under the same experimental conditions.

Quartz Index (QI) = Im/Iq x 100

This value represents the content of quartz (weight %) in the sample only for quartz, and it means a relative amount for other minerals. However, if the strongest X-ray intensity of the pure mineral, Ip, is known, the mineral's content, Cm, can be calculated from the following equation.

Cm (wt, %) = QI x Iq/Ip

When the results of the X-ray analysis are represented by the quartz index, it is possible to make a quantitative comparison of mineral contents among samples. However, drawbacks of this method are as follows:

1) Since the X-ray intensity varies according the degree of crystallization, even if it is a pure substance, the value of quartz index also varies according to the degree of crystallization.

2) In the case of clay minerals or minerals having a cleavage, it gives a larger value than its actual value due to orientation.

3) In the case of poorly-crystallized minerals such as clay minerals, the index may gives a smaller value than the amount of the mineral contained.

In spite of such drawbacks as above method, the QI method is more objective and quantitative, compared with such qualitative representations as large, medium and small.

In the Otake and the Hatchobaru geothermal fields in Oita Prefecture, Japan, quartz index has been applied as follows:

1) Classification of alteration ratio
(wholly altered, mostly altered, half-altered, partially altered, unaltered),

2) Classification of alteration type
(to be described in detail in the following paragraph),

3) Presumption of reservoir cracks
(QI is larger than 50),

4) Presumption of original rocks,

5) Presumption of depth of debris ejected from wells.

Especially in the last case, it is possible to presume the depth of ejected debris with a relatively high degree of accuracy by comparing the QI of each mineral.

(2) Classification of alteration type

Altered rocks can be classified into the following five types, I through V, according to the crystal chemical characteristics of alteration minerals.

Type I:	Silica mineral type
Type II:	Alunite type
Type III:	Kaolin-pyrophyllite type
Type IV:	Alumino-clay type
Type V:	Zeolite-alkalifeldspar type

Basides if mostly altered rock, half-altered rock and partially altered rock and collectively classified into as Type VI and unaltered rock into Type VII, hydrothermal alteration can be systematically represented.

Hydrothermal alteration means the chemical and mineralogical change of rock by geothermal fluid, therefore the order of alteration types corresponds to the order of "alteration degree" or "alteration strength". In other words, it can be said that Type I is the strongest alteration, Type II is strong alteration, Type III is intermediate alteration, Type IV is weak alteration and Type V is very weak alteration. The final classification of alteration should be expressed as strongest alteration-low temperature type, weak alteration-high temperature type, or strongest alteration type-230°C, intermediate alteration type-125°C after estimating the alteration temperature by some method.

The characteristics of each type are outlined below.

1) Type I (strongest alteration type)

This type contains more than 50% (weight) silica minerals produced

by alteration, and forms in the center of the conduit of geothermal fluid. Consequently, this is the most important alteration type to find out geothermal reservoirs or the upward conduit of geothermal fluid Although this type can be formed under both neutral and alkaline conditions, it is apt to be formed under acidic conditions. The main minerals are cristobalite and quartz, and the former is converted into the latter at about 100°C.

2) Type II (strong alteration type)

This type is characterized by the formation of sulfate which has a hexagonal crystal structure such as alunite, and indicates sulfuric acid condition. This type is also formed around the upward conduits of geothermal fluid or outlets of geothermal fluid to the surface, therefore, it becomes a good indicater know the geothermal structures.

3) Type III (intermediate alteration type)

This type is characterized by the formation of kaolin minerals and pyrophyllite, and indicates acidic conditions. In ascending order of temperature, the mineral assemblage is converted from halloysite through kaolinite, to kaolinite + pyrophyllite, or dickite pyrophyllite.

4) Type IV (weak alteration type)

This type is characterized by the formation of montmorillonite, chlorite, mica and interstratified clay minerals, but this type has no zeolite and feldspar. This type is formed in the surroundings of acidic alteration zones, in many cases. Hot water from the Type IV alteration zone is weakly acidic or neutral, although its example is very few. As the alteration temperature increases, the mineral assemblage changes from montmorillonite though chlorite/montmorillonite interstratified mineral to chlorite + mica/montmorillonite interstratified mineral to chlorite + mica. Since pure mica without expandable layers is formed at a temperature higher than 250°C, mica can be used as an indicater for geothermal exploration.

5) Type V (very weak alteration type)

This type is characterized by the formation of zeolite or feldspar and in most cases it is accompanied by clay minerals of Type IV. This type is

formed under neutral or alkaline conditions. It is interesting that this type is recognized in almost all geothermal areas of the world. The pH of hot water from most reservoirs of Type V is neutral to alkaline. However, acidic type of altered veins is, of course, acidic. Mineral change by increasing of temperature is complicated, but it generally is performed in such order as heulandite, laumontite, wairakite, Na-feldspar and K-feldspar.

(3) Standard for classification of alteration type

In accordance with the standard for classification, given in the following list, which was prepared based on the above quartz index, QI, and the concept of classification of alteration type, alteration zonation was carried out. This classification of alteration type has been prepared from much data obtained from the Otake and Hatchobaru geothermal fields, and it is useful for estimating the amounts of altered minerals, the positions of faults, the nature of reservoirs.

Standard for alteration type

Type I (Silica mineral type)

The QI of quartz is larger than 50 (acidic alteration), but in the case of neutral or weak alkaline alteration, larger than 30.

Type II (Alunite type)

Alteration type other than Type I, and alunite is formed.

Type III (Kaolin-phrophyllite type)

Alteration type other than Type I and II, and kaolin and/or phrophyllite are formed.

Type IV (Alumino-clay type)

Alteration type other than Type I, II, III and V, and montmorillonite, chlorite, etc. are formed. However, the total QI of relic minerals is not larger than 5.

Type V (Zeolite-alkalifeldspar type)

Alteration type other than Type I, II and III, and zeolite or alkaline feldspar are formed.

Type VI (Partial alteration)

Alteration type other than I through V type.

Type VII (Unaltered type)

Altered minerals are not formed.

(4) Instrumentation

ME-311 x-ray diffractometer (Toshiba)

(5) Preparation of samples and measurement

Each collected specimen is crushed to a powder of 50 to 100 mesh in a stainless steel mortar and then further ground in an agate mortar until (60 to 240 mesh) coarse particles are not felt by fingers. Each powder sample is packed into an aluminum holder. The experimental conditions are as follows.

Target	Cu
Filter	Ni
Voltage	30 kV
Current	10 mA
Divergence Slit	1°
Receiving Slit	0.2 mm
Scanning Speed	2°/min
Chart Speed	2 cm/min

A.4.4 Method of fracture analysis in core

The survey which the dip and strike of the fracture in the core is important survey to know the geological structure of the area and to estimate the passage of hot water in the subsurface.

In this analysis, the orientation of the core is determined using the natural remanent magnetization of rocks and the dip and strike are measured. The procedure for measurement is shown in the following flow chart.

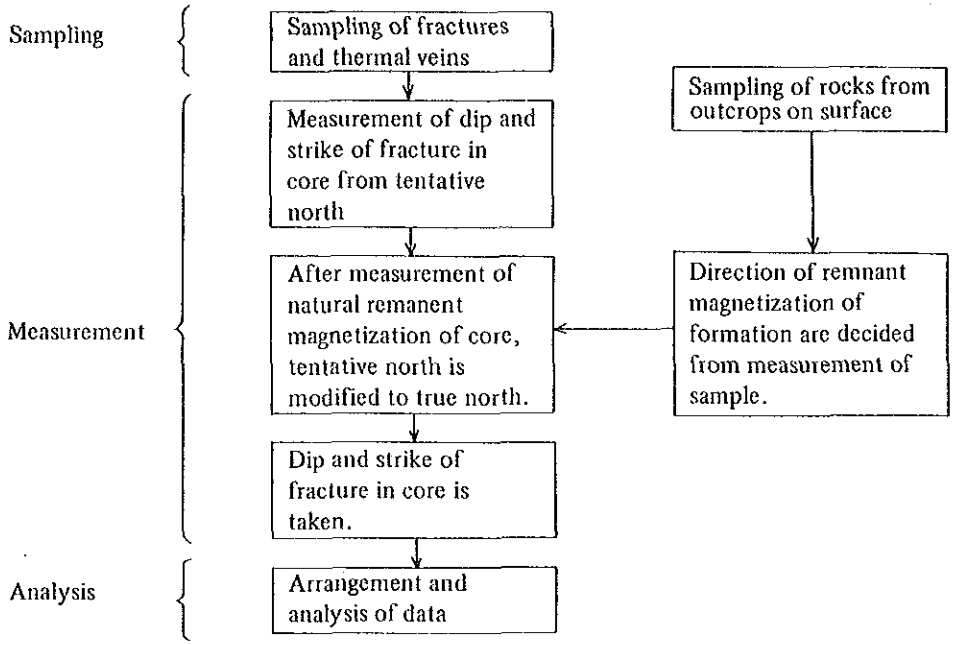

Flow chart of fracture analysis in core

A.4.5 Method of measurement of homogenization temperature of fluid inclusions

(1) Introduction

Fluid inclusion thermometry is effective in gaining information on the present subsurface temperature around the well because it is a quick, easy and cheap method.

Using the hydrothermal minerals collected from cores and cuttings, the fluid inclusion homogenization temperature is measured, and the temperature at which the mineral was formed is determined.

In active geothermal fields, the minimum homogenization temperature at each depth, appears to be almost equal to the present subsurface temperature.

(2) Principle of measurement

Fluid inclusions are the fluids which have been trapped in some way in a crystal during or after the crystal growth. When fluids are trapped in crystals, three kinds of conditions of fluids can be considered:

(a) liquid only
(b) gas only
(c) mixture of liquid and gas

Principally cases (a) and (b) are used to determine the temperature, but case (b) may often include case (c). Then, case (a) is usually applied to determine temperature, since case (b) requires more attention to observation. However, the cases (b) and (c) can be applied to know the boiling phenomenon of the fluid, since the two cases indicate that the fluid was once two phase condition, gas and liquid, or gas along when the fluid was trapped.

As for case (a), i.e. fluid trapped in a crystal is liquid, the principal of fluid inclusion thermometry will be mentioned assuming that the trapping fluid is pure water (refer to Fig. A.4.1). Here we assume that the trapping temperature is 301.5°C at 200 bar, then the density of the water is 0.732 g/cm^3

With decreasing temperature after trapping water, the pressure of the water in an inclusion decreases along an isochoric line of 0.732 g/cm^3 and reaches a saturated pressure line at point HT (290°C, 74.5 bar). When the fluid inclusion reaches at 290°C, it begins to produce steam bubble. On further cooling, the volume of the steam in the inclusion gradually increases with decreasing temperature, keeping the pressure on the saturation line at that temperature. At a certain temperature, the vapor volume ratio to the whole volume of the inclusion is given by following equation:

$$\frac{V_g}{V} = \frac{\rho\ell T_{ob} - \rho\ell T_{ft}}{\rho\ell T_{ob} - \rho g T_{ob}} \qquad \cdots\cdots\cdots\cdots\cdots\cdots\cdots\cdots \quad (1)$$

where V is whole volume of the fluid inclusion, Vg is the volume of the steam phase, $\rho\ell T_{ob}$ is the density of the liquid phase at a certain observation temperature, $\rho g T_{ob}$ the density of the gas phase at the same temperature, and $\rho\ell T_{ft}$ is the density of the liquid phase at the trapping temperature. Now observation is made at 25°C, $\rho g\ 25°C \ll 1$. Therefore equation (1) can be approximated as follows:

$$\frac{V_g}{V} \fallingdotseq 1 - \frac{\rho\ell T_{ft}}{0.9971} \qquad \cdots\cdots\cdots\cdots\cdots\cdots\cdots\cdots \quad (2)$$

Consequently, if the steam ratio can be obtained precisely at 25°C, its (Th) point can be determined. However, it is usually difficult to obtain the steam ratio.

On the other hand, the measurement of a fluid inclusion temperature is carried out in reverse order to the above mentioned. On heating the inclusion, steam

phase gradually becomes smaller until finally it disappears to form only a liquid phase in the inclusion. This temperature is called the homogenization temperature (point Th in Fig. A.4.1). As shown in Fig. A.4.1, the homogenenization temperature (Th point) is different from the formation temperature at which the water was trapped (Tt point). If the trapping pressure of the fluid is known, a correct fluid temperature can be obtained by calculation (pressure correction), but it is usually difficult to know the fluid pressure. However, based upon the consideration of fluid pressure in some active geothermal fields, it is concluded that the fluid pressure in an active geothermal field is not compressed so far from the saturation pressure of water at that temperature, then, pressure correction will not be required. Therefore, the homogenization temperature (Th) can be regarded as the fluid temperature (Tt) in active geothermal fields.

(3) Sample preparation

Minerals such as quartz and anhydrite are desired for the measurement. In the case of calcite, much attention should be paid to the inclusions, since there are such problems that calcite is easily produced at the boiling of solution and there is a possibility of leakage of a part of inclusion due to cleavage.

Transparent crystal grains are selected, and both sides of the samples are polished down to a thickness of 0.2 to 0.7 mm after mounting on a glass slide. It is recommended that the available size of the doubtly polished sample is less than 5 mm x 5 mm. If a sample has an area larger than that size, it should be cut into a smaller size after polishing. Some anhydrite and quartz which are small in size and have clear surfaces can be often used without polishing.

(4) Measuring instrument

Measuring instrument consists of:

Control unit	(FP-80, Mettler Co.)
Heating stage	(FP-82, Mettler Co.)
Microscope	(OPTIPHOT-POL, Nikon)

This instrument can measure temperatures ranging from -20°C to +300°C.

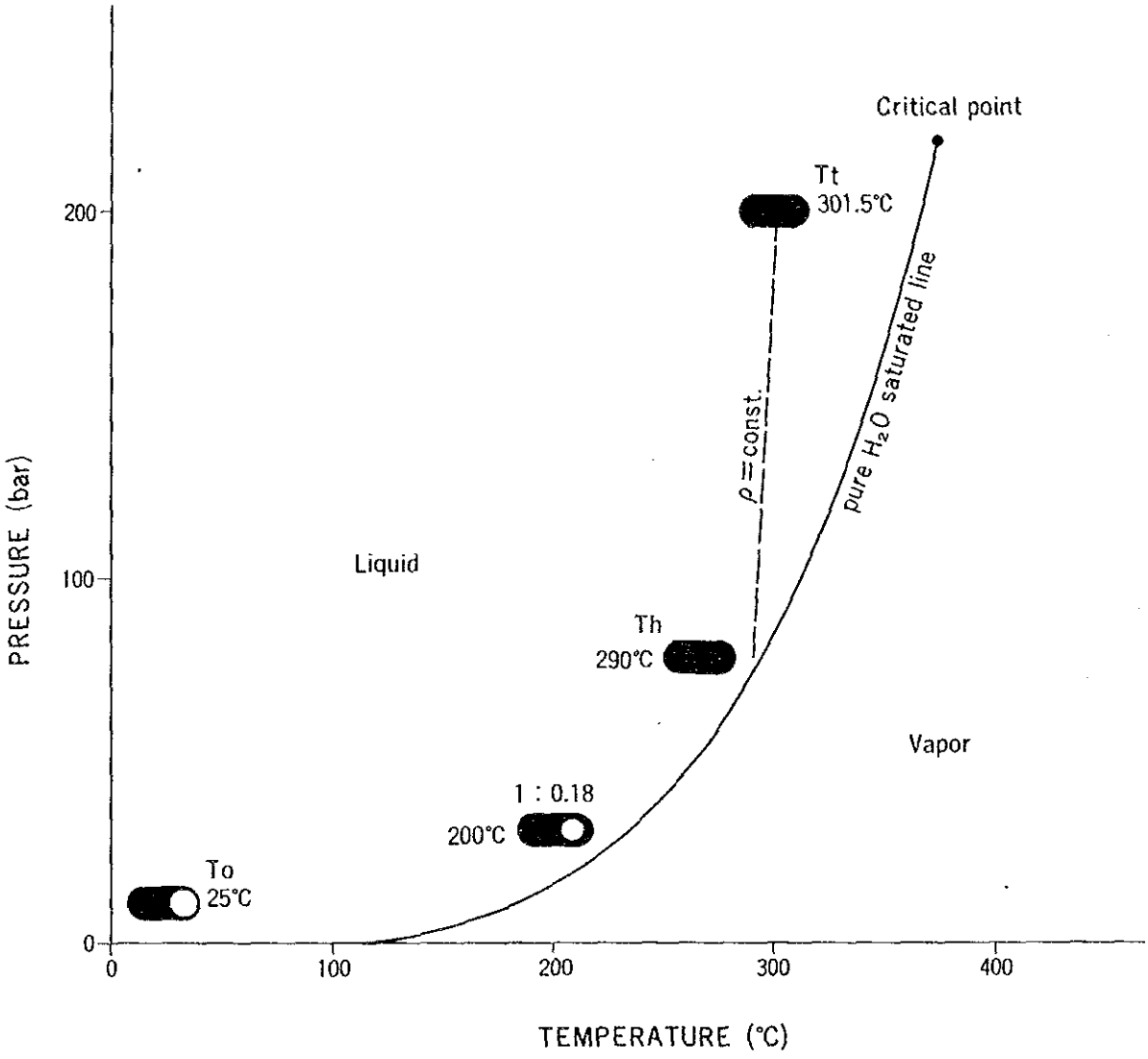

Tt : trapping temperature Th : homogenization temperature
To : observation temperature

Fig. A.4.1 Principles of the fluid inclusion thermometry

(5) Measuring method

The prepared sample is placed on a gloss side and it is inserted into the heating furnace. The sketch of shape, size and distribution of the inclusions are made, and some of the inclusions are photographed.

The sample is heated rapidly up to a temperature about 30°C lower than the homogenization temperature which is presumed from the steam ratio of the inclusion. The sample is then heated step by step at about 10°C intervals to obtain an approximate homogenization temperature. After obtaining the approximate temperature, it is cooled down to a temperature 30°C lower than the approximate one, and the temperature is held until the steam phase appears again in several minutes. Next, the sample is heated again rapidly up to a temperature 10°C lower than the approximate temperature, then a heating rate of 3°C/min. or less is applied up to the homogenization temperature to obtain a precise value. When the inclusion is heated under the condition of a temperature higher than 250°C in the Mettler's heating stage, the cooling air intake beneath the fan of the stage should be sealed off, and the heating rate lower than 1°C/min. is applied.

(6) Representation of results of measurements

The results of measurement of homogenization temperature of fluid inclusions are summarized and listed in the data table of fluid inclusions together with the sampling depth, mineral species, occurrence, measurement number, size and so on.

The table is summarized according to the following criteria.

1) All homogenization temperatures of the primary inclusion which are considered to indicate the formation temperature of minerals should be listed.

2) The temperatures of secondary inclusions which were trapped after the formation of minerals should be listed, if it is considered that the temperatures indicate the temperature of the geothermal fluid at that trapping time.

3) The inclusion classifications by mode of origin into primary and secondary are made on typical ones, and the other inclusions of vague origins are not required to classify unreasonably.

4) Gas rich inclusions should not be measured since they do not usually show the fluid temperature at the time of trapping.

A.4.6 Method of measurement of rock physical properties

(1) Density and porosity

The measurement procedure is as follows:

1) The rock samples are cut into a cylinder 50 mm in diameter and 50 to 60 mm in length. The sample is immersed in water for more than 24 hours. After that, the submerged water-saturated weight is measured. The sample is removed from the immersion bath, the surface dried with a moist cloth and the water-saturated weight is measured.

2) The sample is dried in an oven to a constant weight at a temperature of 105°C for more than two days and allowed to cool in a dessicator. After the oven-dry weight is measured.

3) Density and prosity are given as follows.

$$\rho d = \frac{W_3}{W_1 - W_2}$$

$$\rho w = \frac{W_1}{W_1 - W_2}$$

$$P = \frac{W_1 - W_3}{W_1 - W_2} \times 100\ (\%)$$

Where, ρd: density of oven dry sample
ρw: density of water-saturated sample
W_1: water saturated weight
W_2: submerged water saturated weight
W_3: oven dry weight
P: porosity

(2) Thermal conductivity

Measurement is carried out by the box probe method of nonconstancy heat ray. In Fig. (A), (B) are presented the construction of the probe and the calculation range of the thermal conductivity. The sequence of measurements is as follows:

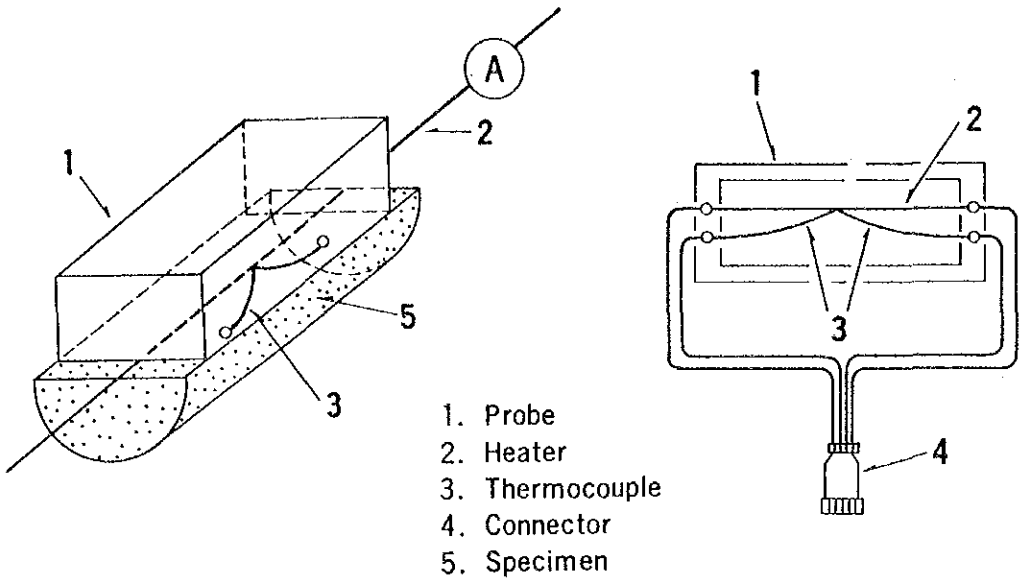

Fig. (A) Construction of probe

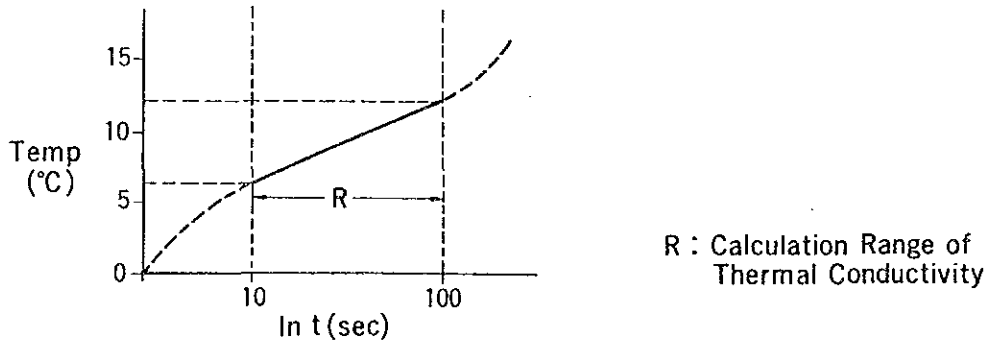

Fig. (B) Relation between time and temperature

1) The samples are cut into a cylinder 50 mm in diameter and 100 mm length under water saturated conditions. They are cut vertically into two sections. The cut surface of one section is ground to a smooth surface using a grinder, and the finished section is used as a specimen for measurement.

2) Prior to measurement, the instrument is adjusted and it is confirmed that its error is within ±3.0% by measuring standard plate (1.183 kcal/m.h.°C). The measurement on the standard plate is carried out for every 5 specimens.

3) Measurements are carried out 3 to 5 times on the same specimen and the results are converted into C.G.S. unit (from kcal/m.h.°C to cal/cm.sec.°C) and an average value is calculated.

4) Thermal conductivity is given as follows:

$$\lambda p = K \cdot \frac{I^2 \ell n(t_2/t_1)}{v_2 - v_1} - H$$

Where, λp: thermal conductivity (Kcal/m.h.°C)
K, H: constant of prove
I: current of heater (A)
v_1, v_2: sampling time
v_1, v_2: output of thermocouple (mv)

(3) Magnetic susceptibility

Measurement of magnetic susceptibility is carried out by the following procedure:

1) The samples are cut into a cylinder 50 mm in diameter and 100 mm length.

2) The instrument is carefully adjusted, then measurements are carried out by the zero method. The instrument is readjusted for every 5 specimens.

3) Magnetic susceptibility of the specimen is obtained from the following formula.

$$K = Q \cdot \frac{Do^2}{D}$$

Where, K: magnetic susceptibility (10^{-6} C.G.S emu)
Q: apparent magnetic susceptibility
Do: standard diameter of instrument (25.4 mm)
D: diameter of specimen (mm)

(4) Resistivity

The measurement procedure is as follows:

1) The samples are cut into a cylinder 50 mm in diameter and divided into 100 mm lengths. Both sides of each piece are polished smooth so that

they become parallel to each other. Fig. (C) shows the outline of resistivity measurement.

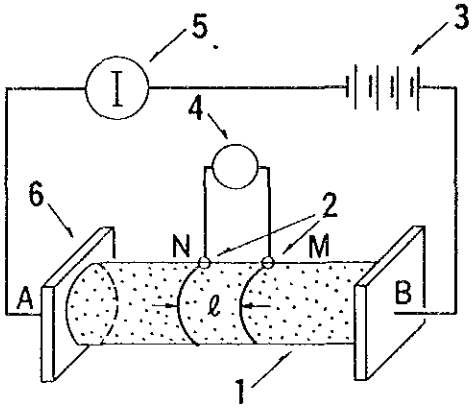

1. Specimen
2. Measuring terminal
3. Stabilized voltage power unit
4. Potentiometer
5. Ammeter
6. Vise

Fig. (C) Outline of resistivity measurement

2) The measurement is carried out by the DC 4-pole method under water saturated conditions.

3) The measuring terminals and a guard terminal to remove the surface current are attached to the specimen using a copper wire of about 0.3 mm in diameter.

4) Conductive silver paste is applied to both sides of the specimen and along the copper wire of all terminals.

5) The specimen is saturated with water following the same procedure as that of the density measurement.

6) The specimen is set in a holder and fixed in a vice.

7) Power is supplied to the specimen and the potential difference between the measuring terminals is determined by a precise DC potentiometer. Measurements are carried out after 5, 10, 15 and 20 minutes. The recorded value of 10 minutes is used as a final value. Resistivity of the specimen is calculated by the following formula.

$$\rho = R \cdot \frac{S}{\ell} = \frac{V}{I} \cdot \frac{S}{\ell}$$

Where, ρ: resistivity to be obtained (Ω.cm)
R: resistance between measuring terminals (Ω)

I: current (A)
V: potential difference between measuring terminals (cm)
S: cross sectional area of specimen (cm^2)
ℓ: length between measuring terminal M and N (cm)

A.5 Results of logging in thermal gradient role

The loggings shown in Table A.5.1 were carried out by MTA. Table A.5.2, Fig. A.5.1 and Fig. A.5.2 show the results of the loggings.

Table A.5.1 List of logging

Well No.	Logging Type	Measured Depth (m)	Date	Remarks
DG–1	Temperature Log (1)	2.50–682.50	26.5.1987	ST = 1 hour
	Temperature Log (2)	5.00–682.50	27.5.1987	ST = 12 hours
	Temperature Log (3)	5.00–682.50	27.5.1987	ST = 24 hours
	Temperature Log (4)	7.50–682.50	28.5.1987	ST = 48 hours
	Temperature Log	3.00– 35.50	–	Drilling depth = 45.50 m
	Temperature Log	2.00–100.50	–	Drilling depth = 100.20 m
	Temperature Log	2.00–250.00	27.4.1987	Drilling depth = 250.00 m
	Temperature Log	2.00–300.00	7.5.1987	Drilling depth = 300.00 m
	Temperature Log	2.00–350.00	8.5.1987	Drilling depth = 351.00 m
	Temperature Log	2.00–398.70	10.5.1987	Drilling depth = 399.00 m
	Temperature Log	5.00–450.00	14.5.1987	Drilling depth = 450.00 m
	Temperature Log	15.00–502.50	17.5.1987	Drilling depth = 502.80 m
	Temperature Log	3.50–550.00	20.5.1987	Drilling depth = 550.40 m
	Temperature Log	0.00–607.50	23.5.1987	Drilling depth = 608.50 m
	Temperature Log	1.50–646.00	24.5.1987	Drilling depth = 646.50 m
	Electrical Log (1)	200.00– 43.00	2.5.1987	
	Electrical Log (2)	682.50– 20.00	26.5.1987	
	Gamma-Ray/Neutron Log	680.00– 2.50	–	
DG–2	Temperature Log (1)	2.00–200.00	8.5.1987	ST = 1 hour
	Temperature Log (2)	0.00–201.00	9.5.1987	ST = 12 hours
	Temperature Log (3)	2.00–200.00	9.5.1987	ST = 24 hours

Well No.	Logging Type	Measured Depth (m)	Date	Remarks
	Temperature Log (4)	2.00–200.00	10.5.1987	ST = 48 hours
	Electrical Log	200.00– 24.00	9.5.1987	
	Gamma-Ray/Neutron Log	0.00–200.50	9.5.1987	
	Density Log	200.00– 0.00	9.5.1987	
DG–3	Temperature Log (1)	0.00–200.50	20.4.1987	ST = 1 hour
	Temperature Log (2)	0.00–200.00	21.4.1987	ST = 12 hours
	Temperature Log (3)	0.00–201.00	21.4.1987	ST = 24 hours
	Temperature Log (4)	0.00–200.00	22.4.1987	ST = 48 hours
	Electrical Log	200.00– 30.00	20.4.1987	
	Gamma-Ray/Neutron Log	0.00–200.50	21.4.1987	
	Density Log	200.00– 0.00	21.4.1987	

Table A.5.2, Results of temperature logging (DG-1)

Depth (m) \ Date	4.'87	27. 4.'87	7. 5.'87	8. 5.'87	10. 5.'87	12. 5.'87	14. 5.'87	17. 5.'87	20. 5.'87	23. 5.'87	24. 5.'87
10	44.2	42.3	48.0	48.0	51.5	52.0	57.5	57.0	61.2	58.0	61.0
20	50.0	46.7	50.3	59.0	56.0	57.5	65.0	62.0	66.0	58.5	66.0
30	63.2	51.0	59.5	66.0	58.0	59.0	68.5	65.2	69.5	66.5	68.5
40	66.6	53.9	58.0	63.5	59.0	61.0	72.5	65.0	71.8	70.0	68.0
50	692(45.5)	56.1	60.0	61.0	61.0	64.3	74.3	73.6	71.5	78.0	68.0
60		59.8	60.3	59.8	61.5	64.3	75.2	73.5	71.6	78.3	78.0
70		62.4	60.3	59.0	62.0	65.0	74.2	74.9	71.7	78.8	79.5
80		64.1	60.3	59.0	62.0	65.0	75.6	74.0	72.1	79.2	79.3
90		65.3	60.3	59.0	62.0	64.0	75.5	74.8	71.9	78.5	79.6
100		66.4	59.5	58.5	61.7	64.3	74.5	73.2	71.8	79.0	79.3
110			60.0	58.5	61.5	64.2	73.9	73.8	72.0	79.0	79.7
120			59.7	58.5	61.5	64.3	74.5	74.6	72.1	79.0	79.7
130			59.7	58.5	61.7	64.0	75.1	73.5	72.2	78.8	79.5
140			59.7	58.8	62.0	64.0	74.5	74.6	72.0	76.8	79.5
150			59.7	58.8	62.0	64.0	74.8	74.5	72.3	78.3	79.6
160			59.7	58.8	62.0	64.0	74.5	73.6	72.2	78.5	79.5
170			59.7	58.5	62.0	64.0	74.6	74.4	72.0	78.4	79.5
180			59.7	58.5	62.0	64.0	74.5	73.8	72.3	78.5	79.5
190			59.7	58.5	62.0	64.0	74.6	74.5	72.5	78.5	79.5
200			59.8	58.2	62.0	64.0	74.4	73.2	72.2	78.0	79.5
210			60.2	58.0	61.5	64.0	74.7	74.5	72.7	78.5	79.4
220			60.3	58.0	61.5	64.0	74.0	74.7	72.7	78.4	79.5
230			60.6	58.0	61.3	64.0	74.5	74.8	73.0	79.3	79.5
240			62.0	58.2	61.3	64.0	74.6	74.8	73.1	78.4	79.4
250			65.5	59.0	61.1	64.3	74.7	74.8	73.2	78.5	79.2
260				59.0	61.2	64.3	74.0	74.8	72.9	78.7	79.3
270				58.0	61.3	64.3	74.6	74.8	73.3	78.7	79.3
280				60.5	61.7	64.3	74.7	74.8	73.3	78.8	79.2
290				60.6	62.0	64.3	74.7	74.8	73.4	78.8	79.8
300				60.5	62.3	64.3	74.7	75.2	72.5	78.9	79.7
310					62.5	64.4	74.7	75.3	74.2	79.4	79.8
320					63.5	64.7	75.3	75.4	73.9	79.0	79.9
330					63.7	65.2	75.5	75.8	74.1	79.0	80.0
340					64.0	65.2	76.0	76.3	75.1	79.2	80.0
350					66.5	65.3	76.1	76.3	75.3	79.4	80.0
360					66.5(351.0)	65.5	76.2	76.3	74.0	79.5	80.2
370						65.7	76.3	76.3	74.9	79.5	80.4
380						65.9	76.9	76.3	75.8	79.6	80.4
390						68.2	77.0	76.3	76.2	79.7	80.5
400						70.0(399.0)	77.0	76.3	76.3	79.7	80.7
410							77.4	76.3	76.3	80.0	80.9
420							77.6	76.4	76.1	80.1	81.0
430							77.8	76.4	76.7	80.2	81.0
440							78.5	76.5	76.7	80.3	81.1
450							79.0	76.5	76.6	80.4	81.2
460								76.5	75.6	80.4	81.3
470								76.6	76.7	80.5	81.4
480								76.7	77.0	81.0	81.5
490								76.8	77.2	81.2	81.6
500								76.9	77.6	81.3	81.6
510								77.0(5028)	78.0	81.4	81.7
520									78.4	81.6	81.8
530									77.5	81.7	82.0
540									79.8	82.0	82.0
550									82.2	82.0	82.0
560										82.3	82.1
570										82.5	82.2
580										83.0	82.4
590										83.2	82.6
600										83.5	82.7
610										836(6085)	82.9
620											83.2
630											83.4
640											83.7
650											839(6465)

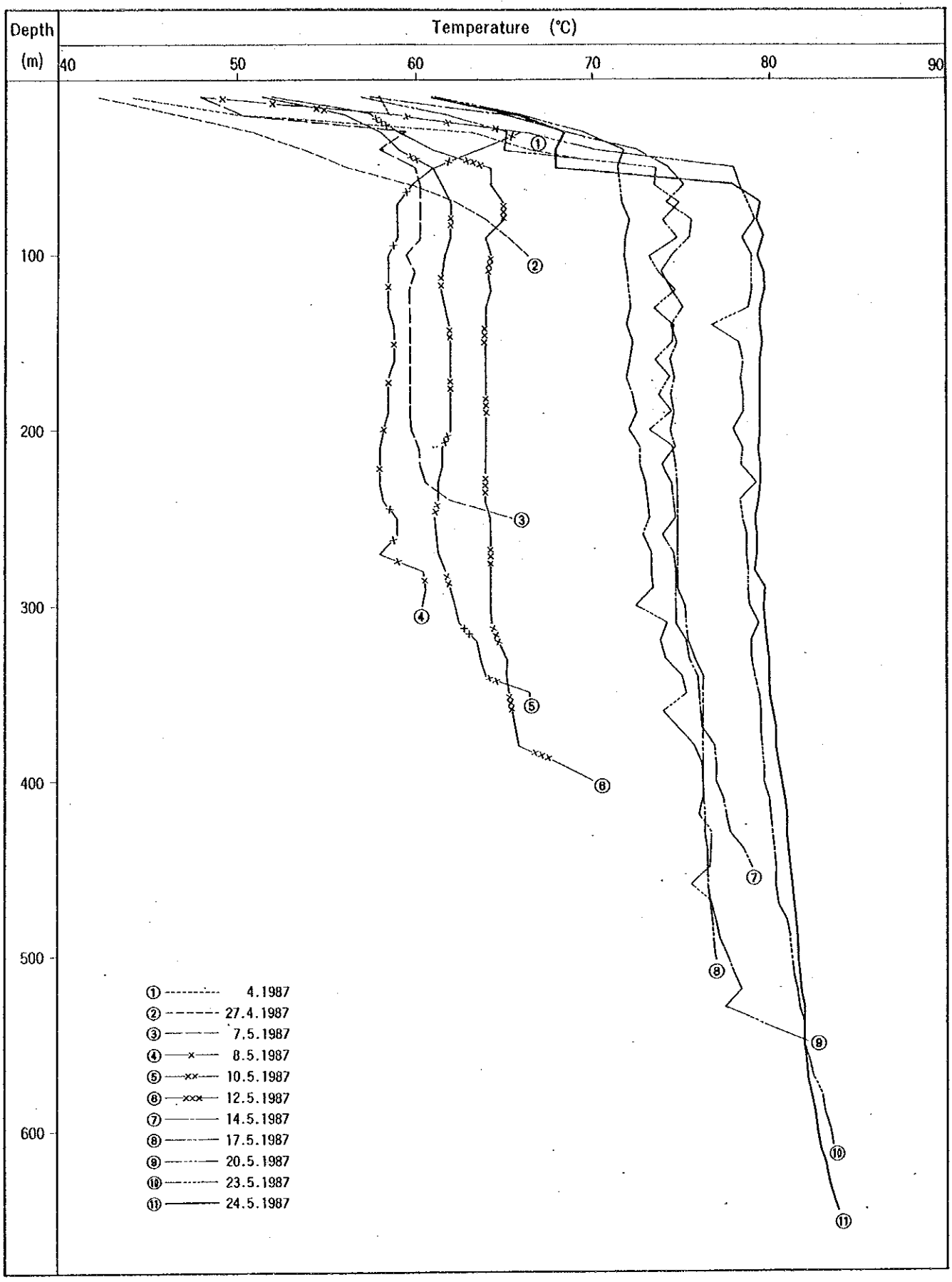

Fig. A. 5. 1 Results of temperature logging (DG−1)

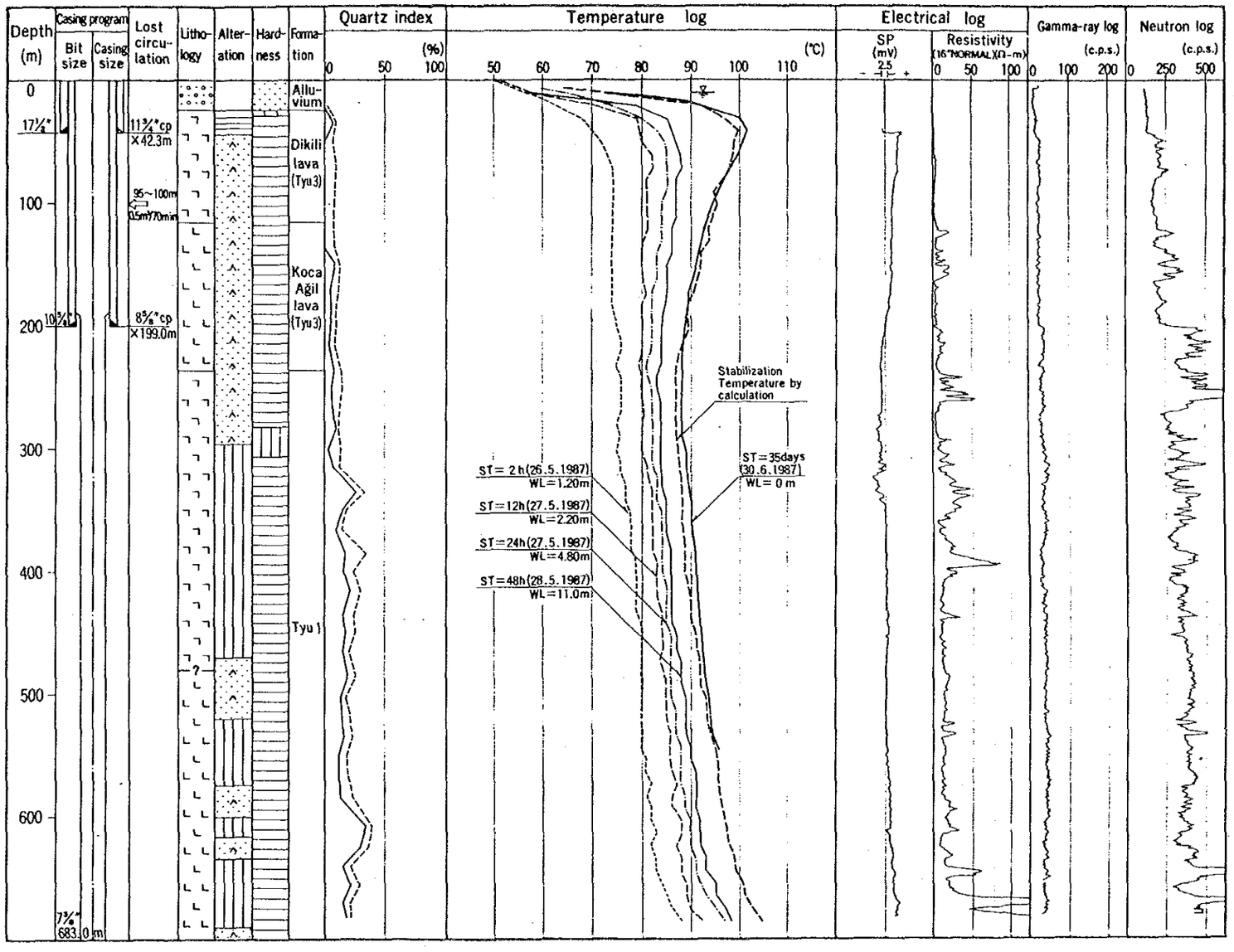

Fig.A.5.2(1) Logging column of DG-1

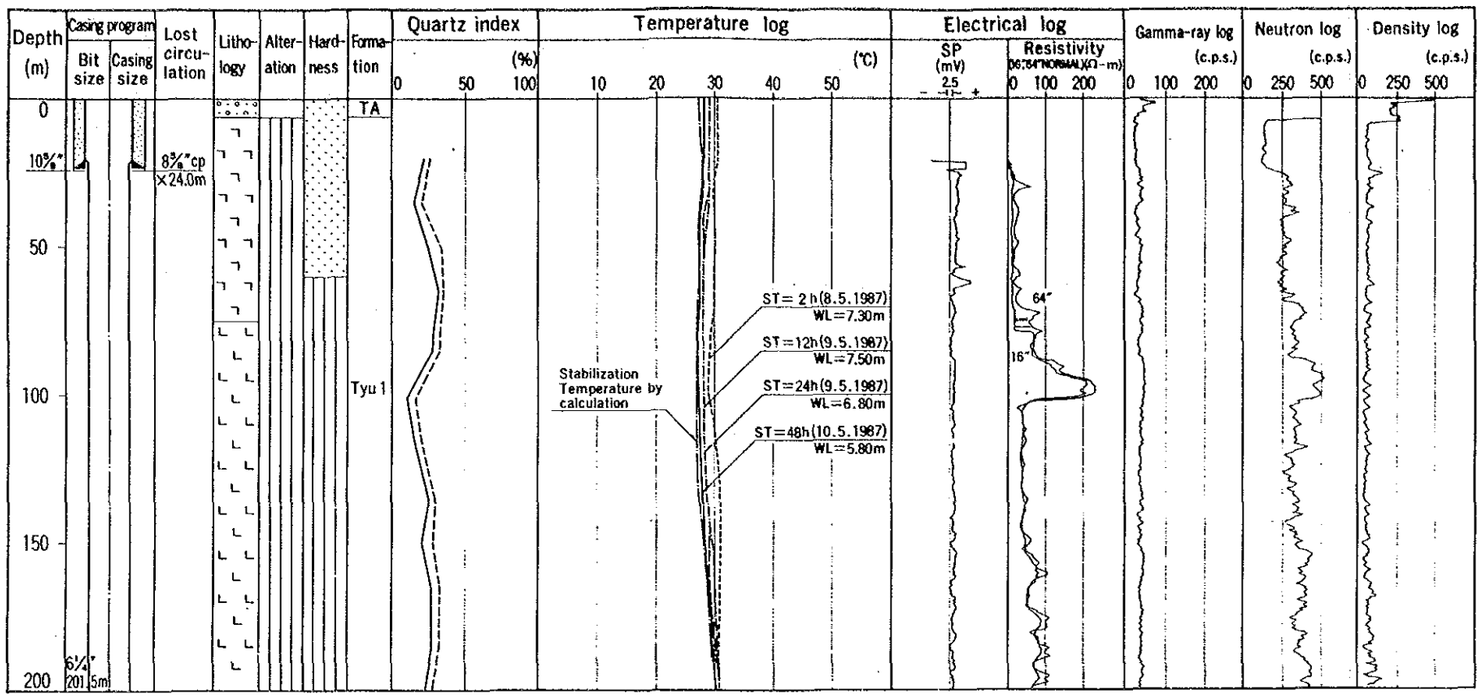

Fig.A.5.2(2) Logging column of DG-2, DG-3